Strong anomalous diffusive behaviors of the two-state random walk process

Jian Liu,[1,*] Ping Zhu,[1] Jing-Dong Bao,[2] and Xiaosong Chen[3]
[1]Department of Physics, Institute of Systems Science, Beijing Technology and Business University, Beijing 100048, China
[2]Department of Physics, Beijing Normal University, Beijing 100875, China
[3]School of Systems Science, Beijing Normal University, Beijing 100875, China

(Received 19 August 2021; revised 1 November 2021; accepted 6 January 2022; published 20 January 2022)

The phenomenon of the two-state process is observed in various systems and is increasingly attracting attention, such that there is a need for a theoretical model of the process. In this paper, we present a prototypal two-state random walk (TSRW) model of a renewal process alternating between the continuous-time random walk (CTRW) state and Lévy walk (LW) state. The jump length distribution of the CTRW state is assumed to be Gaussian whereas the time distributions of the two states are both considered to follow a power law. The diffusive behavior is analyzed and discussed by calculating the mean squared displacement (MSD) analytically and numerically. The results reveal that it displays strong anomalous diffusive behaviors caused by random motions of both states, i.e., two anomalous diffusion terms coexist in the expression of the MSD, and the time distribution which has the heavier tail determines their forms. Moreover, because the two diffusion terms originate from different mechanisms, we find that the diffusion can be characterized by either the term with the largest diffusion exponent or the term with the largest diffusion coefficient at long timescales, which shows very different properties from the single-state process. In addition, the two-state nature of the process of the particle moving in a velocity field makes the TSRW model applicable to describe it. Results obtained from the two-state model reveal that the diffusion can even exhibit subdiffusive behavior, which is significantly different from known results obtained using the single-state model.

DOI: 10.1103/PhysRevE.105.014122

I. INTRODUCTION

Since it was presented by Montroll and Weiss [1,2], the continuous-time random walk (CTRW) theory, which recently completed a 50-year history [3], has proved to be a useful and powerful method and has been widely applied in the study of anomalous transport phenomena in physical, biological, and geological systems [4–8]. As a typical phenomenological model, the CTRW is characterized by the jump length and the waiting time of a walker between two successive jumps, which are both drawn from a joint probability density function (PDF) $\psi(x,t)$, where $\lambda(x)=\int_0^\infty dt\,\psi(x,t)$ is the jump length PDF and $\omega_r(t)=\int_{-\infty}^\infty dx\,\psi(x,t)$ is the waiting-time PDF. It has been extensively observed that anomalous diffusion emerges if the waiting time follows a power law; i.e., $\omega(t)\sim t^{-(1+\alpha)}$ for large t with $0<\alpha<2$. For $0<\alpha<1$, subdiffusion occurs, which is extensively observed in biological systems [9–14]; for $1<\alpha<2$, experimental and theoretical research indicates that anomalous diffusion can be found in complex geological porous media [15–18].

Another fundamental notion in physics and the widely applied phenomenological model is the Lévy walk (LW), whose distinctive feature is the space-time correlation [7,8,19–22]. In the LW scheme, with a constant velocity but a random direction, the particle performs ballistic excursion for a random time interval. After finishing this excursion, the particle immediately randomly chooses a new direction and moves for another random time interval with the same velocity [7]. Instead of jump length and waiting time in the CTRW model, the velocity v of the particle and the time spent in each jump, which is sampled from jump time PDF $\omega_j(t)$, are the two characteristics, which can incorporate the coupled transition PDF,

$$\phi(x,t)=\tfrac{1}{2}\delta(|x|-vt)\omega_j(t), \tag{1}$$

which implies that only particles jumping from $x-vt$ and $x+vt$ can reach x in time interval t and change their velocities after this jump; i.e., the jump size is penalized by the jump time [7]. If the jump time PDF follows a power law $\omega_j(t)\sim t^{-(1+\beta)}$ for large t with $0<\beta<2$, ballistic diffusion ($0<\beta<1$) and subballistic diffusion ($1<\beta<2$) occur. Despite its simplicity, the LW model is able to describe stochastic transport in various areas of research, e.g., the spreading of cold atoms in optical lattices [23,24], dynamics of blinking nanocrystals [25,26], migration of swarming bacteria [27], light transport in special optical materials [28], and foraging patterns of animals [29]. See Ref. [7] for a detailed discussion of the existing applications and current status of the LW model.

When performing the LW, the particle always moves with consecutive velocity renewals. However, if the processes are interrupted by periods of immobilization (rest events) at the turning points, it is the Lévy walk with rests (LWR) model, which is actually a two-state process [7,8,30,31]. The waiting time of the rest event is obtained from an independent

*Corresponding author: liujian@mail.bnu.edu.cn

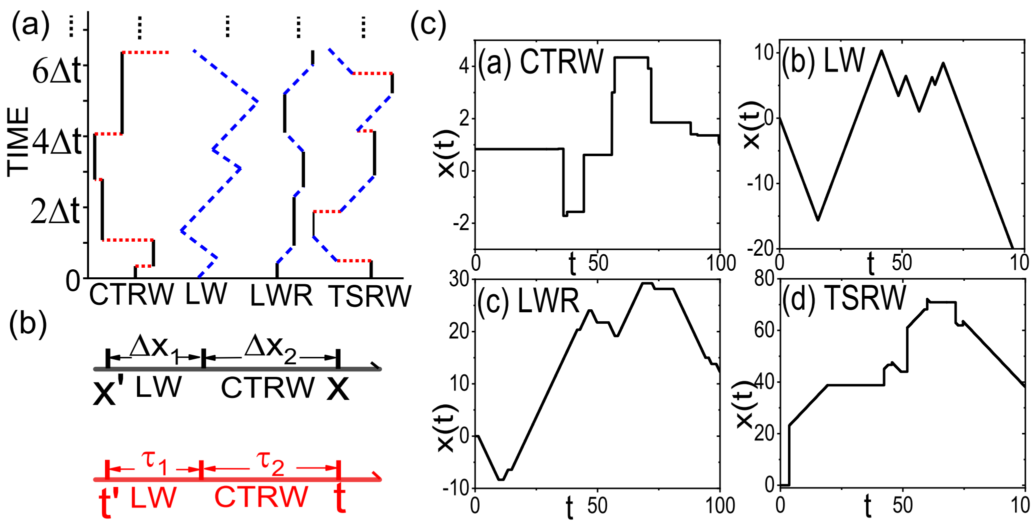

FIG. 1. (a) Schematic descriptions of the CTRW, LW, LWR, and TSRW. The solid black lines denote the waiting times, the dotted red lines denote the instantaneous jump lengths, and the short dashed blue lines denote the Lévy walk steps. (b) Schematic description of the transition process. (c) Numerical realization of the single trajectory of various random walk models, where the applied parameters are $\alpha = 0.6$ and $\sigma = 1.0$ for the CTRW model; $\beta = 0.7$ for the LW model; $\alpha = 0.6$ and $\beta = 0.8$ for the LWR model; $\alpha = 0.8$, $\beta = 0.6$, and $\sigma = 10$ for the TSRW model.

distribution which may be exponential or follow a power law. Competition between the LW excursions and rests can thus affect the time dependence of the mean squared displacement (MSD), e.g., the motion becomes slower than ballistic and subballistic motion. The two-state process can be found in various systems. Trapping occurs when a trajectory undergoes an LW process in a Hamiltonian dynamical system [30,32]. The transport of the neuronal messenger ribonucleoprotein (mRNP) in neuronal systems undergoes an LW process interrupted by rests [33]. The intermittent search strategy clearly exhibits a two-state process which includes a slow local Brownian search phase which is responsible for detecting the target and a fast ballistic excursion phase which aims to relocate into unvisited regions to avoid oversampling [34,35].

Consider that a particle precedes a random diffusion. After being placed in an environment which drives the particle to execute an LW process, the particle's diffusion then comes from the contribution of not only the particle's intrinsic diffusion itself but also the LW resulting from the environment. For example, the mRNP may undergo a local intracellular random transport itself (such as Brownian motion). After being activated by messenger ribonucleic acid, the mRNP stochastically travels along the microtubules bidirectionally until it is captured by target synapses. A more precise example is the intermittent search strategy mentioned above, which includes a local Brownian motion phase and LW phase. Undoubtedly, the mRNP's local intracellular random transport and local Brownian motion of the intermittent search process can be both well described by the CTRW model.

In this paper, we present a renewal two-state process alternating between CTRW and LW, which is called the two-state random walk (TSRW) model. Different from another two-state LWR model, when the particle is in the rest state, the intrinsic random motion which can be well described by the instantaneous jump length of the CTRW is considered. In other words, the waiting time and jump length of the CTRW are dedicated to the rest event and local random motion, respectively, and the LW process is devoted to the ballistic excursion. See Fig. 1(a) for a schematic description of the TSRW model and other existing random walk models.

The remainder of the paper is organized as follows. The TSRW model is presented and the propagator is calculated in Sec. II. Anomalous diffusive behaviors are analyzed and discussed in Sec. III. With the aid of the TSRW model, the diffusion of a particle traveling in a velocity field is discussed in Sec. IV. A summary is given in Sec. V.

II. THE MODEL

We restrict ourselves to the one-dimensional case. Consider that the particle initially stays and rests for a period which is drawn from the corresponding waiting time PDF $\omega_r(\tau_2)$, and then makes an instantaneous random jump which is drawn from the corresponding jump length PDF $\lambda(\Delta x_2)$. The particle then enters the LW state: With a constant velocity v but a random direction with equal probability, the particle keeps walking for a random period drawn from the jump time PDF $\omega_j(\tau_1)$; apparently, the excursion in this walk is $\Delta x_1 = \pm v\tau_1$. After completing the LW state, the particle enters the CTRW state and the process iterates. It can be seen that the propagator $P(x,t)$, which represents the PDF of finding the particle at position x at time t, includes two phases, namely, resting and jumping, i.e., $P(x,t) = P_r(x,t) + P_j(x,t)$, where $P_r(x,t)$ is the PDF of resting and $P_j(x,t)$ is the PDF of jumping.

Indeed, when the particle is in the CTRW state, instead of making only one jump, one can expect that the particle may undergo numerous random steps in real systems. For example, for the intermittent search strategy, there are a number of Gaussian-distributed random searches in the local Brownian motion phase [34,35]. Undoubtedly, these random steps can be meticulously described using, for example, the Langevin picture. While in the framework of the CTRW model which is the typical phenomenological method, these random steps can be statistically and safely described by one jump length.

Define $\eta(x,t)$ as the flux of particles which just finished the CTRW state and started moving out of position x and entering the LW state; it satisfies

$$\eta(x,t) = \int_{-\infty}^{\infty} dx' \int_0^t d\tau_1 \int_0^{t-\tau_1} d\tau_2 \eta(x',t')\phi(\Delta x_1,\tau_1) \times \lambda(\Delta x_2)\omega_r(\tau_2) + \omega_r(t)P_0(x), \tag{2}$$

in which $P_0(x) = P(x,0)$ denotes the initial condition, $\eta(x',t')$ denotes the flux at x' at earlier time t', and it shall accomplish its following LW state and CTRW state to arrive at x at time t, see Fig. 1(b). The second term of the right-hand side of Eq. (2) relates the fact that the particles gradually leave their initial positions according to the waiting time PDF. Considering that $t - t' = \tau_1 + \tau_2$ and $x - x' = \Delta x_1 + \Delta x_2$, and inserting Eq. (1) into Eq. (2) yields

$$\eta(x,t) = \frac{1}{2}\int_{-\infty}^{\infty} dx' \int_0^t d\tau_1 \int_0^{t-\tau_1} d\tau_2 \eta(x', t-\tau_1-\tau_2)\omega_j(\tau_1) \times [\lambda(x-x'+v\tau_1) + \lambda(x-x'-v\tau_1)]\omega_r(\tau_2) + \omega_r(t)P_0(x) \tag{3}$$

and

$$\eta(k,s) = \frac{\omega_r(s)P_0(k)}{1-\frac{1}{2}[\omega_j(s+ivk)+\omega_j(s-ivk)]\omega_r(s)\lambda(k)}, \tag{4}$$

in Fourier-Laplace space, in which the Fourier-Laplace technique $f(k,s) = \mathscr{FL}\{f(x,t)\} = \int_{-\infty}^{\infty} dx \int_0^{\infty} dt e^{-ikx-st} f(x,t)$ is applied.

The propagator $P_r(x,t)$ and $P_j(x,t)$ then can be given by

$$P_r(x,t) = \int_{-\infty}^{\infty} dx' \int_0^t d\tau_1 \int_0^{t-\tau_1} d\tau_2 \eta(x',t')\phi(\Delta x_1,\tau_1) \times \lambda(\Delta x_2)\Phi_r(\tau_2) + \Phi_r(t)P_0(x) \tag{5}$$

and

$$P_j(x,t) = \int_{-\infty}^{\infty} dx' \int_0^t dt' \eta(x',t')\Phi_j(\Delta x_1,\tau_1), \tag{6}$$

in which $\Phi_r(t) = 1 - \int_0^t dt'\omega_r(t')$ is the survival probability of the CTRW state, the probability of not leaving until time t, $\Phi_j(x,t) = \frac{1}{2}\delta(|x| - vt)\Phi_j(t)$, is the survival probability of the LW state, and the probability of moving a distance x and remaining in the state of traveling, $\Phi_j(t) = 1 - \int_0^t dt'\omega_j(t')$, is parallel to the meaning of $\Phi_r(t)$. The first term on the right-hand side of Eq. (5) is the sum of all possible neighboring fluxes at different times, weighted by the coupled transition PDF $\phi(\Delta x_1,\tau_1)$ and jump length PDF $\lambda(\Delta x_2)$, provided the particles survived for a time period τ_2 after their arrival at x at $t-\tau_2$, see Fig. 1(b). The second term on the right-hand side of Eq. (5) accounts for the particles that initially stay at $(x,0)$ and wait until time t to leave. The right-hand side of Eq. (6) relates the sum of all possible neighboring flux which enters the LW state from (x',t'), performs the excursion $\Delta x_1 = x - x'$ with time $\tau_1 = t - t'$, but still remains in the LW state.

After performing the Fourier-Laplace transform on Eqs. (5) and (6) and inserting Eq. (4) into them, they arrive at

$$P_r(k,s) = \frac{\Phi_r(s)P_0(k)}{1-\frac{1}{2}[\omega_j(s+ivk)+\omega_j(s-ivk)]\lambda(k)\omega_r(s)} \tag{7}$$

and

$$P_j(k,s) = \frac{\omega_r(s)\Phi_j(k,s)P_0(k)}{1-\frac{1}{2}[\omega_j(s+ivk)+\omega_j(s-ivk)]\lambda(k)\omega_r(s)}. \tag{8}$$

Correspondingly, the propagator $P(k,s)$ is

$$P(k,s) = P_r(k,s) + P_j(k,s) = \frac{\Phi_r(s) + \Phi_j(k,s)\omega_r(s)}{1-\frac{1}{2}[\omega_j(s+ivk)+\omega_j(s-ivk)]\lambda(k)\omega_r(s)}, \tag{9}$$

in which $\delta(x)$ at $t = 0$ being the initial condition is taken into account.

In this paper, we consider that the waiting time PDF $\omega_r(t)$ and jump time PDF $\omega_j(t)$ both follow a power law,

$$\omega_r(t) \sim \alpha\tau_0^{\alpha} t^{-(1+\alpha)}, \quad 0 < \alpha < 2,$$
$$\omega_j(t) \sim \beta\tau_0^{\beta} t^{-(1+\beta)}, \quad 0 < \beta < 2, \tag{10}$$

for $t \gg \tau_0$, where τ_0 is the microscopic timescale (scaling factor). For long-time limit $t/\tau_0 \to \infty$, the Laplace form of Eq. (10) reads

$$\omega_r(s) = 1 - \tau_\alpha s^{\alpha}, \quad 0 < \alpha < 1,$$
$$\omega_j(s) = 1 - \tau_\beta s^{\beta}, \quad 0 < \beta < 1, \tag{11}$$

and

$$\omega_r(s) = 1 - T_\alpha s + \tau_\alpha s^{\alpha}, \quad 1 < \alpha < 2,$$
$$\omega_j(s) = 1 - T_\beta s + \tau_\beta s^{\beta}, \quad 1 < \beta < 2, \tag{12}$$

in which $\tau_\alpha = |\Gamma(1-\alpha)|\tau_0^{\alpha}$, $\tau_\beta = |\Gamma(1-\beta)|\tau_0^{\beta}$, $T_\alpha = \alpha\tau_0/(\alpha-1)$, and $T_\beta = \beta\tau_0/(\beta-1)$. If the power exponent $\alpha, \beta \in (0,1)$, the mean of $\omega_r(t)$ and $\omega_j(t)$ diverges, the distribution displays distinct asymptotic property. While, if $\alpha, \beta \in (1,2)$, the mean of $\omega_r(t)$ and $\omega_j(t)$ is finite, which is T_α and T_β, respectively, but the variance still diverges, which implies that the distribution displays a weak asymptotic property. Indeed, the time distribution with power exponent belonging to (0,1) displays quite different properties from the one with the power exponent belonging to (1,2) [7,8,36]. For example, to describe the transport of a biased spreading packet in disordered systems, within the CTRW scheme, a fractional advection-diffusion-asymmetry equation has been recently presented, in which a remarkable feature is that the long-tailed PDF of trapping times, which for power exponent belonging to (0,1) implies a fractional time derivative, is transplanted into a spatial space derivative when power exponent belonging to (1,2).

The jump length PDF $\lambda(x)$ is considered to be Gaussian,

$$\lambda(x) = \frac{1}{\sqrt{2\pi\sigma^2}} \exp\left[-\frac{x^2}{2\sigma^2}\right], \tag{13}$$

in which σ^2 is the variance of jump length. For $\sigma^2 = 0$, the intrinsic random motion vanishes and the CTRW state becomes

TABLE I. The specific values of the diffusion exponents of the TSRW model.

Specific cases	$0<\beta<\alpha<1$	$0<\alpha<\beta<1$	$1<\alpha<2, 1<\beta<2$	$1<\alpha<2, 0<\beta<1$	$0<\alpha<1, 1<\beta<2$
Eq. (17)	$\sim t^2 + \sim t^{\beta}$	$\sim t^{2+\alpha-\beta} + \sim t^{\alpha}$	$\sim t^{3-\beta} + \sim t^{1}$	$\sim t^2 + \sim t^{\beta}$	$\sim t^{2+\alpha-\beta} + \sim t^{\alpha}$
Eq. (21)	$\sim t^2 + \sim t^{\frac{2\beta}{\mu}}$	$\sim t^{2+\alpha-\beta} + \sim t^{\frac{2\alpha}{\mu}}$	$\sim t^{3-\beta} + \sim t^{\frac{2}{\mu}}$	$\sim t^2 + \sim t^{\frac{2\beta}{\mu}}$	$\sim t^{2+\alpha-\beta} + \sim t^{\frac{2\alpha}{\mu}}$

a mere rest state, and the TSRW model reduces to the LWR model.

By numerical realization, the single trajectory of the TSRW model is depicted in Fig. 1(c); for comparison, trajectories of other random walk models are also displayed. In this paper, the numerical calculation is implemented adopting the Monte Carlo trajectory-simulating technique [37] along with the number of trajectories $N = 5\times 10^4$, time step $\Delta t = 10^{-3}$, and the velocity $v = 1$. We choose $\omega_r(t) = \alpha\tau_0^{\alpha} t^{-(1+\alpha)}, t \geqslant \tau_0$, and $\omega_j(t) = \beta\tau_0^{\beta} t^{-(1+\beta)}, t \geqslant \tau_0$, and $\tau_0 = 1$ for the numerical simulations. See Appendix C for the details of the numerical simulations.

III. ANOMALOUS DIFFUSIVE BEHAVIORS AND DISCUSSIONS

A. Anomalous diffusive behaviors

In the following, we focus on the diffusive behavior of the process depicted by the TSRW model, which can be obtained from calculating $\langle x^n(t)\rangle = i^n\mathscr{L}^{-1}\{\frac{\partial^n}{\partial k^n}P(k,s)\}_{k=0}$, e.g.,

$$\langle x(t)\rangle = i\mathscr{L}^{-1}\left\{\frac{\partial P(k,s)}{\partial k}\right\}_{k=0} \tag{14}$$

and

$$\langle x^2(t)\rangle = -\mathscr{L}^{-1}\left\{\frac{\partial^2 P(k,s)}{\partial k^2}\right\}_{k=0}, \tag{15}$$

and the MSD $\langle\Delta x^2(t)\rangle = \langle x^2(t)\rangle - \langle x(t)\rangle^2$ are obtained. Apparently, without consideration of bias, $\langle x(t)\rangle = 0$ and $\langle\Delta x^2(t)\rangle = \langle x^2(t)\rangle$. Note that, for the coupled random walk models, the order in which the limits $|k|\to 0$ and $s\to 0$ are performed usually matters [38]. A reasonable consideration is first the limit of small k and then the limit $s \ll 1$ in calculating the asymptotic form of the MSD, which is applied in this paper.

As stated above, the time distribution with the power exponent $\alpha,\beta\in(0,1)$ decays much slower than that with $\alpha,\beta\in(1,2)$. When performing the calculations, we notice that the values of α and β determine the role and the form of local random motion of the CTRW state and ballistic excursion of the LW state in expressing the MSD, which can be specifically categorized into four cases: $0<\alpha<1, 0<\beta<1$; $1<\alpha<2, 1<\beta<2$; $1<\alpha<2, 0<\beta<1$; and $0<\alpha<1, 1<\beta<2$. After completing the calculations, we also find that the results actually can be generally reformed into two cases: $0<\min\{\alpha,\beta\}<1$, and $1<\min\{\alpha,\beta\}<2$. See Appendix A for the detailed calculations and results.

Based on the calculations, the propagator can be expressed as

$$\begin{cases} P(k,s) \simeq \frac{1}{s}\frac{\tau_{\min\{\alpha,\beta\}}s^{\min\{\alpha,\beta\}} - bs^{\beta-2}k^2}{\tau_{\min\{\alpha,\beta\}}s^{\min\{\alpha,\beta\}} + ds^{\beta-2}k^2+\sigma^2k^2}, & 0<\min\{\alpha,\beta\}<1 \\ P(k,s) \simeq \frac{1}{s}\frac{(T_\alpha+T_\beta)s - bs^{\beta-2}k^2}{(T_\alpha+T_\beta)s+ds^{\beta-2}k^2+\sigma^2k^2}, & 1<\min\{\alpha,\beta\}<2, \end{cases} \tag{16}$$

in which $\tau_{\min\{\alpha,\beta\}}$ dedicates τ_β (if $\alpha>\beta$) or τ_α (if $\alpha<\beta$), $b=\frac{1}{2}|(\beta-1)(\beta-2)|\tau_\beta v^2$, and $d=\frac{1}{2}|\beta(\beta-1)|\tau_\beta v^2$. Correspondingly, the expression of the MSD can be asymptotically expressed as

$$\langle\Delta x^2(t)\rangle \simeq \begin{cases} D_1 t^{2-\beta+\min\{\alpha,\beta\}} + D_1' t^{\min\{\alpha,\beta\}}, & 0<\min\{\alpha,\beta\}<1 \\ D_2 t^{3-\beta} + D_2' t, & 1<\min\{\alpha,\beta\}<2, \end{cases} \tag{17}$$

in which $D_1 = (1-\beta)v^2$ for $\alpha>\beta$ or $D_1 = \frac{2|1-\beta|\tau_\beta v^2}{\Gamma(3+\alpha-\beta)\tau_\alpha}$ for $\alpha<\beta$, $D_1' = \frac{2\sigma^2}{\Gamma(1+\beta)\tau_\beta}$ for $\alpha>\beta$ or $D_1' = \frac{2\sigma^2}{\Gamma(1+\alpha)\tau_\alpha}$ for $\alpha<\beta$, $D_2 = \frac{2(\beta-1)\tau_\beta v^2}{\Gamma(4-\beta)(T_\alpha+T_\beta)}$, and $D_2' = \frac{2\sigma^2}{T_\alpha+T_\beta}$. The specific values of the diffusion exponent are displayed in Table I. Actually, the first term on the right-hand side of Eq. (17) originates from LW state (the LW term) and the second one originates from CTRW state (the CTRW term) [39]. In other words, the LW state and CTRW state each plays its own role in contributing the diffusion. In addition, consider that the LW term possesses the bigger diffusion exponent, which should be the leading term at large timescales, and the MSD can be approximately expressed by

$$\langle\Delta x^2(t)\rangle \propto \begin{cases} t^{2-\beta+\min\{\alpha,\beta\}}, & 0<\min\{\alpha,\beta\}<1 \\ t^{3-\beta}, & 1<\min\{\alpha,\beta\}<2 \end{cases} \tag{18}$$

at large timescales.

Moreover, though the form of Eq. (17) can be classified as a LW term and CTRW term, it can be seen that the time distribution (with the smaller power exponent) of the two states which decays slower determines its expression. For the

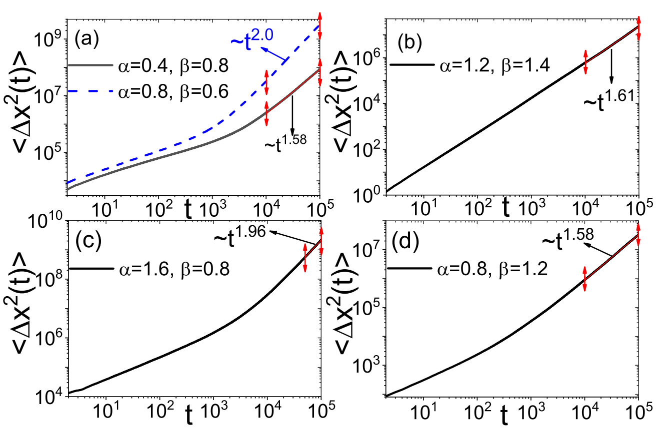

FIG. 2. MSD $\langle \Delta x^2(t) \rangle$ as a function of time t with various α and β. (a) $0 < \alpha < 1$, $0 < \beta < 1$, which includes $0 < \beta < \alpha < 1$ and $0 < \alpha < \beta < 1$; (b) $1 < \alpha < 2$, $1 < \beta < 2$; (c) $1 < \alpha < 2$, $0 < \beta < 1$; (d) $0 < \alpha < 1$, $1 < \beta < 2$. The asymptotic diffusive behaviors (i.e., the diffusion exponents from the linear fit) are in good agreement with the theoretical results at large timescales. The parameters applied in the numerical simulations are $\sigma = 100$, $\sigma = 1$, $\sigma = 100$, and $\sigma = 10$ for the four subgraphs.

CTRW state (with $0 < \min\{\alpha, \beta\} < 1$), the MSD is $\sim t^\alpha$ for $\alpha < \beta$ and $\sim t^\beta$ for $\alpha > \beta$. For the LW state, if $\alpha < \beta$, different from the pure LW process, it is not ballistic diffusion $\sim t^2$ $(0 < \beta < 1)$ and subballistic diffusion $\sim t^{3-\beta}$ $(1 < \beta < 2)$, it is $\sim t^{2+\alpha-\beta}$ instead, which can even behave as subdiffusion if $\beta - \alpha > 1$. The long traps of the CTRW state drastically affect the diffusion of the LW state, which is supposed to be the super one.

With medium σ, considering various α and β, which are on behalf of the cases stated in Eqs. (17) and (18), the MSDs $\langle \Delta x^2(t) \rangle$ varying with time t are displayed in Fig. 2. It can be seen that since more than one diffusive process coexists at an intermediate timescale, crossover appears in between the diffusion processes. However, as expected, the crossover is always followed by a steady state which is characterized by the biggest exponent, just as given in Eq. (18). Crossover phenomena can be observed in various systems as long as there is more than one diffusive process or mechanism in the evolutions, for example, intracellular transport in biological systems [10], the transport of granular gases in a homogeneous cooling state or glass-forming liquids [40,41], correlated CTRW transporting in a velocity field [42,43], and anomalous diffusion of correlated Lévy flight [44].

B. Discussions

1. Comparison with LWR model

Indeed, the asymptotic diffusive behavior Eq. (18) is exactly the same as the LWR model; the ballistic excursion of the LW and time distribution with a smaller power exponent jointly determine the diffusion's asymptotic behavior [8]. This is not surprising and is understandable. As is known, diffusion is characterized in the limit of a large timescale, and the term with the largest diffusion exponent prevails in the expression of MSD. Since the jump length PDF of the CTRW state is the trivial Gaussian distribution while the LW state performs ballistic excursion, the diffusion originating from the CTRW state cannot compete with the diffusion from the LW state—the diffusion exponent of CTRW term is always smaller than the one of the LW term. Hence, the diffusion of the CTRW state may contribute at the intermediate timescale but the MSD's asymptotic behavior is always determined by the LW state (and time distribution with smaller exponent).

However, we want to mention that considering the bifractional characteristic of the TSRW model (the two fractional diffusions originate from different mechanisms), it can display quite different phenomena from the LWR model: instead of the diffusion exponent, diffusion can be temporarily characterized by the diffusion coefficient even at large timescales and does not obey the previous definition. In addition, the state occupation caused by the time distribution with the smaller exponent of the two states can determine its final behavior at ultimate large timescales. In this sense, the CTRW state may dominate in the TSRW process; see below. Besides, after considering bias, the diffusion of the CTRW state also becomes very important; see Sec. IV.

2. The role of diffusion coefficient

Compared with the velocity $v = 1$, medium and large σ is applied in numerically depicting the single trajectory of the TSRW process, which is displayed in Fig. 3(a)—the applied exponents are $\alpha = 0.6$ and $\beta = 0.8$. For the medium σ such as $\sigma = 1$, $\sigma = 10$, and $\sigma = 10^2$, the CTRW state and LW state can be easily distinguished, but for the large σ such as $\sigma = 10^4$ (in this case, $D_1' \gg D_1$ and $D_2' \gg D_2$), the LW state has become indistinguishable. Surely, the LW state is not kind of being erased, but suppressed by strong fluctuations of the CTRW state. The MSDs varying with time are depicted at the same time, which is displayed in Fig. 3(b). It can be seen that for medium σ, the diffusion exponents are all well consistent with the expected value $2 + \alpha - \beta$ at large timescales, i.e., the diffusion exponent of the LW term in Eq. (17). However, for large σ such as $\sigma = 10^4$, even at large timescales, the diffusion exponent is contrarily consistent with the diffusion exponent of the CTRW term.

Apparently, for $\sigma = 10^4$, instead of the LW term which has the largest diffusion exponent, the diffusion is characterized by the CTRW term which has the largest diffusion coefficient, which does not obey the previous conclusion. The intrinsic reason is the two-state nature of the the TSRW model. Specifically speaking, the CTRW term and LW term originate from different mechanisms: If one mechanism fluctuates so strongly that the corresponding diffusion coefficient is much larger than the other one, the process originating from the other mechanism can be suppressed. Then, in contrast with expressing the diffusion using the LW term having the largest diffusion exponent, the diffusion can be expressed using the CTRW term which has the largest diffusion coefficient.

Stochastic transport disturbed by multiple origins can be widely observed in physical and biological systems [42,43,45–49]. Take an active particle's random intracellular transport, for example: The stochastic motion comes from not only thermal agitation from the surroundings, but also the actively fluctuating forces such as the (de)polymerization of cytoskeletal filaments, the active motion of molecular

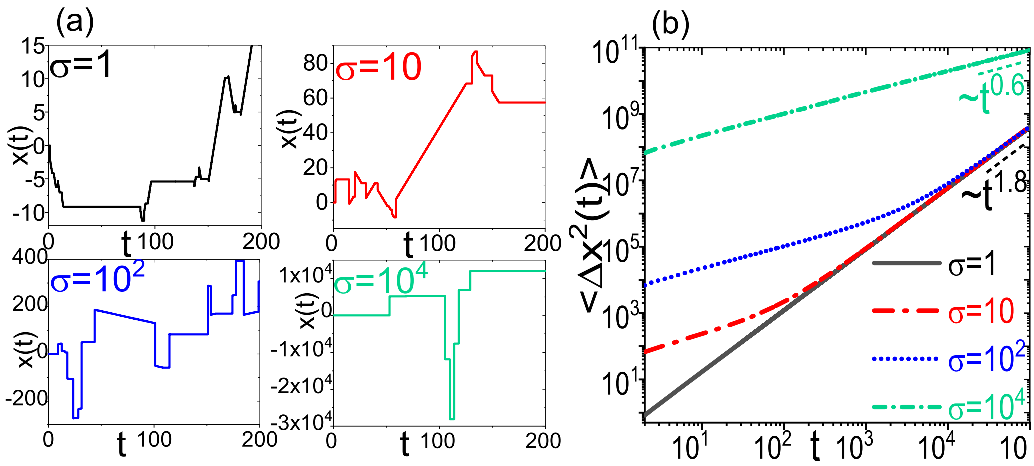

FIG. 3. The applied exponents are $\alpha = 0.6$ and $\beta = 0.8$. (a) Single trajectory of the TSRW process with various σ. For $\sigma = 10^4$, the LW state becomes very hard to distinguish. (b) MSD $\langle \Delta x^2(t) \rangle$ as a function of time t with various σ. For $\sigma = 1, \sigma = 10$, and $\sigma = 10^2$, the diffusion exponents from linear fit are well consistent with the expected value $2 + \alpha - \beta$ (the diffusion exponent of the LW term), whereas, for $\sigma = 10^4$, the diffusion exponent is consistent with α (the diffusion exponent of the CTRW term).

motors along these filaments, and the kinesin-driven transport of cargo along linear microtubule tracks [46–48]. In healthy cells, transport of cargo can be maintained to almost behave as ballistic motion, however, it is not strong enough and usually covered by other effects, and the diffusion behaves as a sub or normal type. Undoubtedly, separating the superdiffusive process from others and studying its transport property, such as the mechanism of preventing and avoiding traffic jams, is meaningful [48,49]. We hope that the TSRW model and the results discussed in this paper could provide some clue for it.

Lastly, we want to stress that, considering the diffusion coefficient is just a constant, diffusion determined by the term which has the largest diffusion coefficient is still just a transient phenomenon, even if it holds for a number of timescales as the results displayed in Fig. 3(b). For extremely long-time limit $t \to \infty$, theoretically, the term which has the largest diffusion exponent can certainly defeat the term which has the largest diffusion coefficient, and finally dominates the diffusion. However, for experimental research, the timescale of this long-last transient phenomenon can go beyond the timescale of the experimental observation and may mislead the research. In this sense, we consider that the TSRW model deserves further study and may be able to help avoid this possible not readily noticeable mistake.

3. Nontrivial jump length

One more thing worthy of discussion is that, instead of Gaussian distribution, if the jump length PDF is considered to be a power law shape, e.g., the Lévy distribution $\lambda(x) \sim \sigma^{-\mu}|x|^{-(1+\mu)}$ whose Fourier form is

$$\lambda(k) = \exp(-\sigma^{\mu}|k|^{\mu}) \simeq 1 - \sigma^{\mu}|k|^{\mu}, \tag{19}$$

with $1 < \mu < 2$ being the Lévy index [50], the diffusion of the CTRW state could be stronger than the LW state. After inserting Eq. (19) into Eq. (9), the following calculations are very similar to the procedure of calculating Eqs. (16) and (17). Following the previous thoughts, the propagator can be expressed as

$$\begin{cases} P(k,s) \simeq \frac{1}{s}\frac{\tau_{\min\{\alpha,\beta\}}s^{\min\{\alpha,\beta\}} - bs^{\beta-2}k^2}{\tau_{\min\{\alpha,\beta\}}s^{\min\{\alpha,\beta\}} + ds^{\beta-2}k^2 + \sigma^{\mu}|k|^{\mu}}, & 0 < \min\{\alpha,\beta\} < 1 \\ P(k,s) \simeq \frac{1}{s}\frac{(T_\alpha + T_\beta)s - bs^{\beta-2}k^2}{(T_\alpha + T_\beta)s + ds^{\beta-2}k^2 + \sigma^{\mu}|k|^{\mu}}, & 1 < \min\{\alpha,\beta\} < 2, \end{cases} \tag{20}$$

and the MSD can be expressed as [51]

$$\langle \Delta x^2(t) \rangle \propto \begin{cases} \sim t^{2-\beta+\min\{\alpha,\beta\}} + \sim t^{\frac{2\min\{\alpha,\beta\}}{\mu}}, & 0 < \min\{\alpha,\beta\} < 1 \\ \sim t^{3-\beta} + \sim t^{\frac{2}{\mu}}, & 1 < \min\{\alpha,\beta\} < 2. \end{cases} \tag{21}$$

The specific values of the diffusion exponent are given in Table I. It can be seen that the second diffusion exponent certainly can be larger than the first one. Considering that the Lévy flight itself is a strong nonlocal diffusive process, we have to say, in this sense, the TSRW model must be describing a drastic fluctuating stochastic process.

IV. DIFFUSION OF THE PARTICLE TRANSPORTING IN A VELOCITY FIELD

A. The diffusive behaviors

One topic relating to the CTRW model is the diffusion of random diffusive particles traveling in a constant velocity field, including the fluid flowing freely and the fluid flowing through porous media [5,42,43,52,53]. In particular, for the latter case, the particle could get stuck in pores or jump out and move freely with the fluid. The scheme of the process described by the CTRW is as follows.

The particle getting stuck in pores implies that it stays at its present position, which can be precisely described by the waiting time. After staying still for a time period, the particle jumps out and accomplishes a jump length, while the jump length shall be corrected by the bias from the velocity field. But in the CTRW theory, each jump is accomplished instantaneously and does not cost any time—the bias from the velocity field in each jump cannot be directly measured. The comprised method is from the viewpoint of clock time of experimental observation (see Fig. 1 of Ref. [42] for the schematic description of the time lines of CTRW), once the particle jumps, it is measured and recorded within the experimental constant time interval Δt, hence the bias μ can be estimated as the product of the fluid's constant velocity v and the constant time interval Δt: $\mu = v\Delta t$. In other words, after staying still for a random waiting time, the following jump length of the particle is corrected by the distance covered by the moving fluid during the measurement time interval Δt.

Compared with the above comprised method, the scheme depicted by the TSRW model may provide a more natural scenario. The random diffusive particle is captured by pores and stays still for a random time period τ_2 drawn from $\omega_r(\tau_2)$, then jumps out and flows with the velocity field for another random time period τ_1 drawn from $\omega_j(\tau_1)$ until it is captured again; the process iterates. Apparently, the excursion in each flowing is just the sum of the particle's intrinsic random fluctuation Δx_2 drawn from the jump length PDF $\lambda(\Delta x_2)$ and the distance traveling with the fluid $\Delta x_1 = v\tau_1$. In this sense, the bidirectional motion of the LW state reduces to the directed one, i.e., instead of Eq. (1), the coupled transition PDF is now expressed as

$$\phi(x,t) = \delta(x - vt)\omega_j(t). \tag{22}$$

After considering Eq. (22) in the expressions of Eqs. (2)–(5), we have

$$\eta(k,s) = \frac{\omega_r(s)P_0(k)}{1 - \omega_j(s+ivk)\omega_r(s)\lambda(k)}, \tag{23}$$

$$P_r(k,s) = \frac{\Phi_r(s)P_0(k)}{1 - \omega_j(s+ivk)\omega_r(s)\lambda(k)}, \tag{24}$$

$$P_j(k,s) = \frac{\omega_r(s)\Phi_j(k,s)P_0(k)}{1 - \omega_j(s+ivk)\omega_r(s)\lambda(k)}, \tag{25}$$

and

$$P(k,s) = \frac{\Phi_r(s) + \Phi_j(k,s)\omega_r(s)}{1 - \omega_j(s+ivk)\lambda(k)\omega_r(s)}, \tag{26}$$

in which $\delta(x)$ at $t = 0$ being the initial condition is still taken into account. Note that if the particle traveling in the velocity field does not have intrinsic random fluctuations, $\sigma^2 = 0$, then the transport of the particle can be precisely described by the directed LWR model.

In the following, we restrict ourselves to the typical asymptotic regime $\alpha, \beta \in (0,1)$; a brief discussion on the other cases is presented in Appendix B 2. For $\alpha, \beta \in (0,1)$, the first moment $\langle x(t)\rangle$ and second moment $\langle x^2(t)\rangle$ are (see Appendix B 1 for detailed derivations)

$$\langle x(t)\rangle \simeq \begin{cases} vt, & \alpha > \beta \\ \frac{\tau_\beta v}{\Gamma(2+\alpha-\beta)\tau_\alpha} t^{1+\alpha-\beta}, & \alpha < \beta \end{cases} \tag{27}$$

and

$$\langle x^2(t)\rangle \simeq \begin{cases} v^2t^2 + \frac{2\sigma^2}{\Gamma(1+\beta)\tau_\beta}t^\beta, & \alpha > \beta \\ \frac{2(1-\beta)\tau_\beta v^2}{\Gamma(3+\alpha-\beta)\tau_\alpha}t^{2+\alpha-\beta} + \frac{2\sigma^2}{\Gamma(1+\alpha)\tau_\alpha}t^\alpha + \frac{2\beta\tau_\beta^2 v^2}{\Gamma(3+2\alpha-2\beta)\tau_\alpha^2}t^{2+2\alpha-2\beta}, & \alpha < \beta, \end{cases} \tag{28}$$

respectively. Correspondingly the MSD can be expressed as

$$\langle \Delta x^2(t)\rangle \simeq \begin{cases} \frac{2\sigma^2}{\Gamma(1+\beta)\tau_\beta}t^\beta, & \alpha > \beta \\ \frac{2(1-\beta)\tau_\beta v^2}{\Gamma(3+\alpha-\beta)\tau_\alpha}t^{2+\alpha-\beta} + \frac{2\sigma^2}{\Gamma(1+\alpha)\tau_\alpha}t^\alpha & \\ + \frac{\tau_\beta^2 v^2}{\tau_\alpha^2}\Big[\frac{2\beta}{\Gamma(3+2\alpha-2\beta)} - \frac{1}{\Gamma^2(2+\alpha-\beta)}\Big]t^{2+2\alpha-2\beta}, & \alpha < \beta. \end{cases} \tag{29}$$

Considering $\sim t^{2+\alpha-\beta}$ is the leading term for the $\alpha < \beta$ case, it can be approximately expressed as

$$\langle \Delta x^2(t)\rangle \simeq \begin{cases} \frac{2\sigma^2}{\Gamma(1+\beta)\tau_\beta}t^\beta, & \alpha > \beta \\ \frac{2(1-\beta)\tau_\beta v^2}{\Gamma(3+\alpha-\beta)\tau_\alpha}t^{2+\alpha-\beta}, & \alpha < \beta \end{cases} \tag{30}$$

at large timescales. For both $\alpha > \beta$ and $\alpha < \beta$ case, the MSDs $\langle \Delta x^2(t)\rangle$ varying with time t are displayed in Fig. 4, it can be seen that the diffusion exponents from numerical simulation are in good agreement with the expected ones at large timescales.

From Eqs. (29) and (30), it can be seen that for the $\alpha > \beta$ case, the MSD behaves as a subdiffusive behavior and the particle's intrinsic random motion (described by the jump length of the CTRW state) plays the key role in expressing the diffusion. This is understandable. For $\alpha > \beta$, $\omega_j(\tau_1)$ dominates the whole process and, consequently, the first moment $\langle x(t)\rangle$ which can only be obtained from the LW state increases linearly with time t, see Eq. (27), and the second moment of LW state is proportional to t^2, see Eq. (28). In other words, the

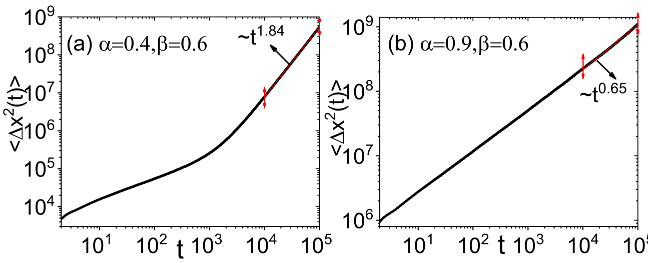

FIG. 4. MSD $\langle \Delta x^2(t) \rangle$ as a function of time t with (a) $\alpha > \beta$, and (b) $\alpha < \beta$. The diffusion exponents from liner fit are all in agreement with the theoretical ones at large timescales. The parameters applied in the numerical simulations are $\sigma = 1000$ and $\sigma = 100$ for the two subgraphs, respectively.

directed excursion of the LW state is only responsible for the particle's standard advection, and the diffusion is only determined by $\lambda(\Delta x_2)$ and $\omega_j(\tau_1)$ especially, i.e., $\langle \Delta x^2(t) \rangle \sim t^{\beta}$. For $\alpha < \beta$, $\omega_r(\tau_2)$ dominates; the longer power law traps of $\omega_r(\tau_2)$ make the first moment obtained from the LW state increase sublinearly with time $\langle x(t) \rangle \sim t^{1+\alpha-\beta}$, which makes the term having the largest diffusion exponent preserved in expressing the MSD, therefore the diffusion is still the subballistic form $\langle \Delta x^2(t) \rangle \sim t^{2+\alpha-\beta}$ at large timescales.

Within the CTRW scheme, the diffusion of the particle moving in the velocity field flowing through porous media is $\langle \Delta x^2(t) \rangle \sim t^{2\alpha}$ [5,42,52,53]. Apparently, the results of the particle moving in the velocity field described by the TSRW model are distinctly different from the results described by the CTRW model. In our opinion, the two-state nature of the process of which the particle moves in the velocity field flowing through porous media makes the TSRW model feasible to describe it. However, we state that the CTRW and TSRW models should both be applicable for the relevant topics, and which one to apply shall depend on the problem studied.

B. Discussions

As mentioned above, if $\sigma^2 = 0$, the process can be precisely described using the directed LWR model; in this case, for $\alpha > \beta$, $\omega_j(\tau_1)$ dominates the whole process, which results in $\langle x(t) \rangle \sim t$ and $\langle x^2(t) \rangle \sim t^2$, and, correspondingly, $\langle \Delta x^2(t) \rangle \sim 0$ for the long-time limit, and the process can be regarded just as a directional flow. For $\alpha < \beta$, $\omega_r(\tau_2)$ dominates, $\sim t^{2+\alpha-\beta}$ is still the leading term in expressing the MSD. Additionally, the discussion on the diffusion coefficient in Sec. III is also applicable in this section; we do not repeat it here. Furthermore, not just limited to the velocity field, any environment which can bring bias, the process can be also described by the TSRW model. In describing the asymmetry, the coupled transition PDF can be expressed as $\phi(x,t) = a\delta(x - vt)\omega_j(t) + (1-a)\delta(x + vt)\omega_j(t)$, $0 \leqslant a \leqslant 1$, in which a measures the asymmetry.

When flowing with the constant velocity field in the directed LW state, one can expect that instead of moving freely with the fluid, the particle may travel in a frictional environment. In this case, the motion in each directed LW state can be described by

$$\dot{x}(t) = v(t), \quad \dot{v}(t) = -\gamma v(t), \tag{31}$$

in which γ describes the friction coefficient. Correspondingly, the excursion in each directed LW step becomes $x = \frac{v}{\gamma}(1 - e^{-\gamma t})$ and, instead of Eq. (22), the coupled transition PDF is now expressed as $\phi(x,t) = \delta[x - \frac{v}{\gamma}(1 - e^{-\gamma t})]\omega_j(t)$.

Considering the long-tailed property of the power law distribution $\omega_j(t)$, the excursion actually can be approximately expressed as $x \simeq \frac{v}{\gamma}$, and the joint transition PDF is $\phi(x,t) \simeq \delta(x - \frac{v}{\gamma})\omega_j(t)$ of which the distinctive space-time correlation feature of LW is actually smoothed out. Instead of the ballistic excursion in each directed LW step, the distance now becomes trivial just like the Gaussian jump length in the CTRW state. In this case, the diffusion is predictable and the MSD has the same scaling as the result described by the CTRW model [5,42,52,53], i.e., the time distribution with the smaller power exponent determines the expression of the MSD: $\langle \Delta x^2(t) \rangle \sim t^{2\min\{\alpha,\beta\}}$. Considering the same α and β which are applied in Fig. 4, the MSDs $\langle \Delta x^2(t) \rangle$ varying with time t are displayed in Fig. 5(a). It can be seen that the diffusion exponents from numerical simulation are in good agreement with the expected ones, which are distinctly different from the results displayed in Fig. 4.

The discussion can be naturally extended to the TSRW model. After considering friction in the LW state, instead of Eq. (1), the coupled transition PDF becomes $\phi(x,t) \simeq \delta(|x| - \frac{v}{\gamma})\omega_j(t)$. Still, the distinctive space-time correlation feature of the LW is smoothed out and the distance in each LW step becomes a trivial term. The diffusion is entirely determined by the time distribution with the smaller power exponent at large timescales, i.e.,

$$\langle \Delta x^2(t) \rangle \sim \begin{cases} t^{\min\{\alpha,\beta\}}, & 0 < \min\{\alpha,\beta\} < 1 \\ t, & 1 < \min\{\alpha,\beta\} < 2. \end{cases} \tag{32}$$

Considering the same α and β applied in Fig. 2, the MSDs $\langle \Delta x^2(t) \rangle$ varying with time t are displayed in Fig. 5(b); it can be seen that the numerical results are in good agreement with Eq. (32) at large timescales, which are distinctly different from the results displayed in Fig. 2.

V. SUMMARY

In this paper, we presented a TSRW model, which is a renewal two-state process alternating between the CTRW state and LW state. The waiting time distribution $\omega_r(t)$ of the CTRW state and the jump time distribution $\omega_j(t)$ of the LW state are both considered to follow power laws with the power exponents $\alpha, \beta \in (0,2)$. By calculating the MSD analytically and numerically, the anomalous diffusive behaviors of this model were discussed. Results revealed that the local random motion of the CTRW state and ballistic excursion of the LW state both contribute the diffusive behaviors in the form of two anomalous diffusion terms (the CTRW term and LW term) coexisting in the expression of the MSD. In addition, we found that the time distribution with the heavier tail dominates and determines the two MSD's forms, especially if $\omega_r(t)$ dominates ($\alpha < \beta$), the ballistic or subballistic diffusion of the LW state can be suppressed by the long traps of the CTRW state, e.g., $\langle \Delta x^2(t) \rangle \sim t^{2+\alpha-\beta}$. Moreover, since the two diffusion terms originate from different mechanisms, the diffusion can be characterized by the LW term which

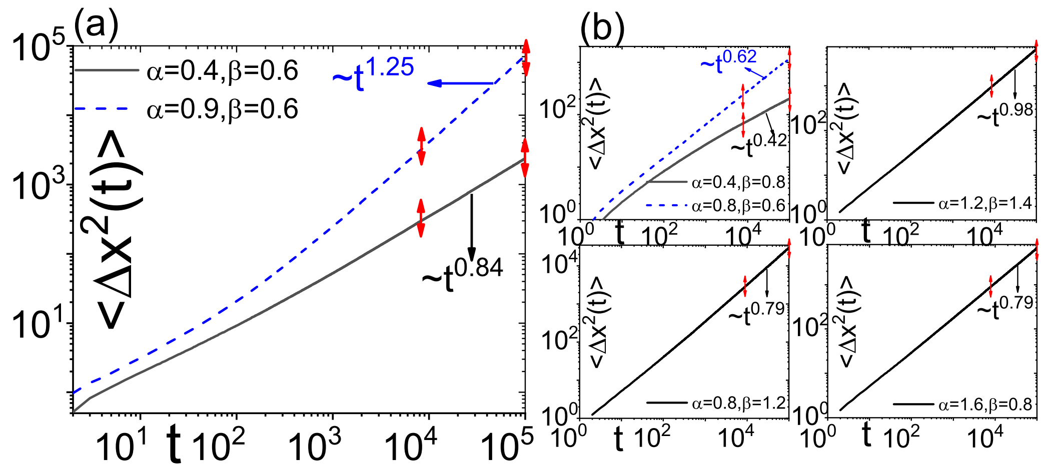

FIG. 5. MSD $\langle \Delta x^2(t) \rangle$ as a function of time t with LW state considering friction. (a) Diffusion of the particle transporting in the velocity field described by the TSRW model; the exponents α and β are the same as the ones applied in Fig. 4. (b) Diffusion of the TSRW model; the exponents α and β are the same as those applied in Fig. 2. The diffusion exponents from linear fit are in good agreement with the expected ones. The applied parameters are $\sigma = 1$ and $\gamma = 1$.

owns the largest diffusion exponent or the CTRW term which owns the largest diffusion coefficient even at large timescales. Such classification of diffusion implies that for realistic systems or experimental observations, the original definition of diffusion, e.g., from a single-state process, is not applicable for the two-state process, and shall draw attention.

Within the TSRW scheme, the diffusion of the particle moving in a velocity field flowing through porous media is discussed. The two-state nature of the process means that the TSRW model can comfortably describe the process. The results reveal that the scenario and the diffusions are distinctly different from the known results depicted by the single-state CTRW model. Still, if $\alpha < \beta$, the long traps of the CTRW state drag out the diffusion of the LW state, but for the $\alpha > \beta$ case, the LW state can only supply a standard advection effect for the process—the diffusion behaves as a subdiffusion determined by the jump length of the CTRW state and jump time of the LW state.

There are more and more two-state processes observed in physical and biological systems [33–35,54,55], of which the single-state model can not flexibly describe them [55]. For now, some two-state models such as the two-state Langevin equation with fast and slow diffusion modes [56,57], the two-state process with Brownian motion and LW [58,59], have been recently presented. We believe that these two-state models including the TSRW model presented in this paper have potential applications in describing the two-state phenomena.

ACKNOWLEDGMENTS

This work is supported by the National Natural Science Foundation of China under Grants No. 11605003 and No. 11735005, and the Support Project of High-level Teachers in Beijing Municipal Universities under Grant No. CIT&TCD201904034.

APPENDIX A: DERIVATION OF EQS. (16)–(18)

Let's first give the expressions of $\lambda(x)$, $\omega_r(t)$, $\omega_j(t)$, $\Phi_r(t)$, and $\Phi_j(x,t)$ in Fourier-Laplace space, which are frequently called in the derivations of Eqs. (16)–(18).

From Eqs. (13), the Fourier form of $\lambda(x)$ can be easily obtained:

$$\lambda(k) = \exp(-\sigma^2 k^2) \simeq 1 - \sigma^2 k^2. \tag{A1}$$

The expression of $\omega_r(s)$ is given in Eqs. (11) and (12), and $\Phi_r(s)$ can be obtained from

$$\Phi_r(s) = \frac{1 - \omega_r(s)}{s}, \tag{A2}$$

correspondingly.

The expressions of $\omega_j(s)$ and $\Phi_j(k,s)$ should take care of the value of β—besides, to calculate the MSD, we are interested in the behaviors of $P(k,s)$ for s fixed and $k \to 0$ [38].

For $0 < \beta < 1$,

$$\omega_j(s+ivk) = 1 - \tau_\beta (s+ivk)^\beta \simeq 1 - \tau_\beta\left[s^\beta + i\beta v s^{\beta-1}k - \tfrac{1}{2}\beta(\beta-1)v^2 s^{\beta-2}k^2\right], \tag{A3}$$

$$\omega_j(s-ivk) = 1 - \tau_\beta (s-ivk)^\beta \simeq 1 - \tau_\beta\left[s^\beta - i\beta v s^{\beta-1}k - \tfrac{1}{2}\beta(\beta-1)v^2 s^{\beta-2}k^2\right], \tag{A4}$$

and, correspondingly,

$$\tfrac{1}{2}\big[\omega_j(s+ivk)+\omega_j(s-ivk)\big]\simeq 1-\tau_\beta s^\beta+\tfrac{1}{2}\beta(\beta-1)\tau_\beta v^2 s^{\beta-2}k^2. \tag{A5}$$

Considering $\Phi_j(x,t)=\frac{1}{2}\delta(|x|-vt)\Phi_j(t)$ and $\Phi_j(t)=1-\int_0^t dt'\omega_j(t')$, and invoking Eqs. (A3) and (A4) at the same time, there is

$$\begin{aligned}\Phi_j(k,s)&=\frac{1}{2}\big[\Phi_j(s+ivk)+\Phi_j(s-ivk)\big]\\&=\frac{1}{2}\bigg[\frac{1-\omega_j(s+ivk)}{s+ivk}+\frac{1-\omega_j(s-ivk)}{s-ivk}\bigg]\simeq\tau_\beta s^{\beta-1}-\frac{1}{2}(\beta-1)(\beta-2)\tau_\beta v^2 s^{\beta-3}k^2.\end{aligned} \tag{A6}$$

For $1<\beta<2$, based on Eq. (12) and similar to the procedure Eqs. (A3)–(A6), we can arrive at

$$\tfrac{1}{2}[\omega_j(s+ivk)+\omega_j(s-ivk)]\simeq 1-T_\beta s+C_\beta s^\beta-\tfrac{1}{2}\beta(\beta-1)C_\beta v^2 s^{\beta-2}k^2 \tag{A7}$$

and

$$\Phi_j(k,s)\simeq T_\beta-C_\beta s^{\beta-1}+\tfrac{1}{2}(\beta-1)(\beta-2)C_\beta v^2 s^{\beta-3}k^2. \tag{A8}$$

As stated in the main text of the paper, the MSD can be calculated from Eqs. (14) and (15), while the value of α and β should be considered. Our calculations can be categorized into four cases: $0<\alpha<1, 0<\beta<1$; $1<\alpha<2, 1<\beta<2$; $1<\alpha<2, 0<\beta<1$; and $0<\alpha<1, 1<\beta<2$. After completing the calculations, we notice that the results actually can be recategorized into two cases: $0<\min\{\alpha,\beta\}<1$; $1<\min\{\alpha,\beta\}<2$. The specific calculations are presented as follows.

1. $0<\alpha<1, 0<\beta<1$

After inserting Eqs. (11), (A1), (A2), (A5), and (A6) into Eq. (9), and after omitting the higher order terms, we have

$$P(k,s)\simeq\frac{1}{s}\frac{\tau_\alpha s^\alpha+\tau_\beta s^\beta-\frac{1}{2}(\beta-1)(\beta-2)\tau_\beta v^2 s^{\beta-2}k^2}{\tau_\alpha s^\alpha+\tau_\beta s^\beta-\frac{1}{2}\beta(\beta-1)\tau_\beta v^2 s^{\beta-2}k^2+\sigma^2k^2}. \tag{A9}$$

By invoking Eq. (15), the MSD can be expressed as

$$\langle\Delta x^2(t)\rangle=\langle x^2(t)\rangle=\mathscr{L}^{-1}\bigg\{\frac{2(1-\beta)\tau_\beta v^2}{s^{3-\beta}}\frac{1}{\tau_\alpha s^\alpha+\tau_\beta s^\beta}+\frac{2\sigma^2}{s}\frac{1}{\tau_\alpha s^\alpha+\tau_\beta s^\beta}\bigg\}. \tag{A10}$$

Indeed, the term $\frac{1}{\tau_\alpha s^\alpha+\tau_\beta s^\beta}$ in Eq. (A10) implies that the asymptotic form of the MSD will be determined by the long-tailed property of $\omega_r(t)$ and $\omega_j(t)$. The following calculations should take care of the value of α and β.

For $\alpha>\beta$,

$$\frac{1}{\tau_\alpha s^\alpha+\tau_\beta s^\beta}=\frac{1}{\tau_\beta s^\beta\big(1+\frac{\tau_\alpha}{\tau_\beta}s^{\alpha-\beta}\big)}\sim\frac{1}{\tau_\beta s^\beta},\quad s\to 0, \tag{A11}$$

and, correspondingly, the MSD can be asymptotically expressed as

$$\langle\Delta x^2(t)\rangle\simeq(1-\beta)v^2t^2+\frac{2\sigma^2}{\Gamma(1+\beta)\tau_\beta}t^\beta. \tag{A12}$$

Since diffusion is characterized in the limit of the large timescale and the term with the largest exponent prevails in the expression of MSD, considering $2>\beta$, the MSD can be approximately expressed by

$$\langle\Delta x^2(t)\rangle\simeq(1-\beta)v^2t^2. \tag{A13}$$

For $\alpha<\beta$,

$$\frac{1}{\tau_\alpha s^\alpha+\tau_\beta s^\beta}=\frac{1}{\tau_\alpha s^\alpha\big(1+\frac{\tau_\beta}{\tau_\alpha}s^{\beta-\alpha}\big)}\sim\frac{1}{\tau_\alpha s^\alpha},\quad s\to 0, \tag{A14}$$

and the MSD can be asymptotically expressed as

$$\langle\Delta x^2(t)\rangle\simeq\frac{2(1-\beta)\tau_\beta v^2}{\Gamma(3+\alpha-\beta)\tau_\alpha}t^{2+\alpha-\beta}+\frac{2\sigma^2}{\Gamma(1+\alpha)\tau_\alpha}t^\alpha. \tag{A15}$$

Considering $2+\alpha-\beta>\alpha$, it can be approximately expressed by

$$\langle\Delta x^2(t)\rangle\simeq\frac{2(1-\beta)\tau_\beta v^2}{\Gamma(3+\alpha-\beta)\tau_\alpha}t^{2+\alpha-\beta}. \tag{A16}$$

Combing Eqs. (A9), (A11), and (A14), the $P(k,s)$ can be expressed as

$$P(k,s) \simeq \frac{1}{s}\frac{\tau_{\min\{\alpha,\beta\}}s^{\min\{\alpha,\beta\}} - bs^{\beta-2}k^2}{\tau_{\min\{\alpha,\beta\}}s^{\min\{\alpha,\beta\}} + ds^{\beta-2}k^2 + \sigma^2k^2}, \tag{A17}$$

in which $\tau_{\min\{\alpha,\beta\}}$ dedicates τ_β (if $\alpha > \beta$) or τ_α (if $\alpha < \beta$), $b = \frac{1}{2}|(\beta-1)(\beta-2)|\tau_\beta v^2$, and $d = \frac{1}{2}|\beta(\beta-1)|\tau_\beta v^2$. Combing Eqs. (A12) and (A15), it is

$$\langle \Delta x^2(t) \simeq D_1 t^{2-\beta+\min\{\alpha,\beta\}} + D_1' t^{\min\{\alpha,\beta\}}. \tag{A18}$$

Combing Eqs. (A13) and (A16), it is

$$\langle \Delta x^2(t) \simeq D_1 t^{2-\beta+\min\{\alpha,\beta\}}, \tag{A19}$$

in which $D_1 = (1-\beta)v^2$ for $\alpha > \beta$, or $D_1 = \frac{2|1-\beta|\tau_\beta v^2}{\Gamma(3+\alpha-\beta)\tau_\alpha}$ for $\alpha < \beta$, and $D_1' = \frac{2\sigma^2}{\Gamma(1+\beta)\tau_\beta}$ for $\alpha > \beta$, or $D_1' = \frac{2\sigma^2}{\Gamma(1+\alpha)\tau_\alpha}$ for $\alpha < \beta$.

2. $1 < \alpha < 2, 1 < \beta < 2$

Similar to the calculations on Eqs. (A9) and (A10), after inserting Eqs. (12), (A1), (A2), (A7), and (A8) into Eq. (9), and after omitting the higher order terms, we have

$$P(k,s) \simeq \frac{1}{s}\frac{(T_\alpha + T_\beta)s - bs^{\beta-2}k^2}{(T_\alpha + T_\beta)s + ds^{\beta-2}k^2 + \sigma^2k^2} \tag{A20}$$

and

$$\langle \Delta x^2(t)\rangle \simeq \mathscr{L}^{-1}\left\{\frac{2(\beta-1)\tau_\beta v^2}{s^{3-\beta}}\frac{1}{(T_\alpha+T_\beta)s} + \frac{2\sigma^2}{s}\frac{1}{(T_\alpha+T_\beta)s}\right\} = D_2 t^{3-\beta} + D_2' t, \tag{A21}$$

in which $D_2 = \frac{2(\beta-1)\tau_\beta v^2}{\Gamma(4-\beta)(T_\alpha+T_\beta)}$ and $D_2' = \frac{2\sigma^2}{T_\alpha+T_\beta}$. Considering $3-\beta > 1$, it can be approximately expressed by

$$\langle \Delta x^2(t)\rangle \simeq D_2 t^{3-\beta}. \tag{A22}$$

3. $1 < \alpha < 2, 0 < \beta < 1$

Still, similar to the calculations in Eqs. (A9) and (A10), after inserting Eqs. (12), (A1), (A2), (A5), and (A6) into Eq. (9), and after omitting the higher order terms, we have

$$P(k,s) \simeq \frac{1}{s}\frac{\tau_\beta s^\beta - bs^{\beta-2}k^2}{\tau_\beta s^\beta + ds^{\beta-2}k^2 + \sigma^2k^2} \tag{A23}$$

and

$$\langle \Delta x^2(t)\rangle \simeq \mathscr{L}^{-1}\left\{\frac{2(1-\beta)\tau_\beta v^2}{s^{3-\beta}}\frac{1}{\tau_\beta s^\beta} + \frac{2\sigma^2}{s}\frac{1}{\tau_\beta s^\beta}\right\} = D_1 t^2 + D_1' t^\beta. \tag{A24}$$

Considering $2 > \beta$, it can be approximately expressed by

$$\langle \Delta x^2(t)\rangle \simeq D_1 t^2. \tag{A25}$$

4. $0 < \alpha < 1, 1 < \beta < 2$

Still, similar to the calculations in Eqs. (A9) and (A10), after inserting Eqs. (11), (A1), (A2), (A7), and (A8) into Eq. (9), and after omitting the higher order terms, we have

$$P(k,s) = \frac{1}{s}\frac{\tau_\alpha s^\alpha - bs^{\beta-2}k^2}{\tau_\alpha s^\alpha + ds^{\beta-2}k^2 + \sigma^2k^2} \tag{A26}$$

and

$$\langle \Delta x^2(t)\rangle \simeq \mathscr{L}^{-1}\left\{\frac{2(\beta-1)\tau_\beta v^2}{s^{3-\beta}}\frac{1}{\tau_\alpha s^\alpha} + \frac{2\sigma^2}{s}\frac{1}{\tau_\alpha s^\alpha}\right\} = D_1 t^{2+\alpha-\beta} + D_1' t^\alpha. \tag{A27}$$

Considering $2+\alpha-\beta > \alpha$, it can be approximately expressed by

$$\langle \Delta x^2(t)\rangle \simeq D_1 t^{2+\alpha-\beta}. \tag{A28}$$

In conclusion, it can be seen that Eqs. (A17), (A23), and (A26) actually can be expressed as

$$P(k,s) \simeq \frac{1}{s}\frac{\tau_{\min\{\alpha,\beta\}}s^{\min\{\alpha,\beta\}} - bs^{\beta-2}k^2}{\tau_{\min\{\alpha,\beta\}}s^{\min\{\alpha,\beta\}} + ds^{\beta-2}k^2 + \sigma^2k^2}, \quad 0 < \min\{\alpha,\beta\} < 1. \tag{A29}$$

Correspondingly, Eqs. (A18), (A24), and (A27) can be expressed as

$$\langle \Delta x^2(t) \simeq D_1 t^{2-\beta+\min\{\alpha,\beta\}} + D_1' t^{\min\{\alpha,\beta\}}, \quad 0 < \min\{\alpha,\beta\} < 1, \tag{A30}$$

and Eqs. (A19), (A25), and (A28) can be expressed as

$$\langle \Delta x^2(t) \simeq D_1 t^{2-\beta+\min\{\alpha,\beta\}}, \quad 0 < \min\{\alpha,\beta\} < 1. \tag{A31}$$

Compared to Eq. (A29), Eq. (A20) now can be expressed as

$$P(k,s) \simeq \frac{1}{s}\frac{(T_\alpha + T_\beta)s - bs^{\beta-2}k^2}{(T_\alpha + T_\beta)s + ds^{\beta-2}k^2 + \sigma^2 k^2}, \quad 1 < \min\{\alpha,\beta\} < 2. \tag{A32}$$

Combining Eqs. (A29) and (A32), Eq. (16) is performed. Combining Eqs. (A30) and (A21), Eq. (17) is performed; combining Eqs. (A31) and (A22), Eq. (18) is performed.

APPENDIX B: DERIVATION OF EQ. (27)–(30)

1. $0 < \alpha < 1, 0 < \beta < 1$

Considering $\Phi_j(k,s) = \Phi_j(s+ivk)$ now, Eq. (25) can be expressed as

$$P(k,s) = \frac{\frac{1-\omega_r(s)}{s} + \frac{1-\omega_j(s+ivk)}{s+ivk}\omega_r(s)}{1-\omega_j(s+ivk)\lambda(k)\omega_r(s)}. \tag{B1}$$

After inserting Eqs. (11), (A1), and (A3) into Eq. (B1), and after omitting the higher order terms, the propagator can be approximately expressed as

$$P(k,s) \simeq \frac{1}{s}\frac{\tau_{\min\{\alpha,\beta\}}s^{\min\{\alpha,\beta\}} + i(\beta-1)\tau_\beta v s^{\beta-1}k - bs^{\beta-2}k^2}{\tau_{\min\{\alpha,\beta\}}s^{\min\{\alpha,\beta\}} + i\beta\tau_\beta v s^{\beta-1}k + ds^{\beta-2}k^2 + \sigma^2 k^2}. \tag{B2}$$

After inserting Eq. (B2) into Eqs. (14) and (15), we have

$$\langle x(t)\rangle = \mathscr{L}^{-1}\left\{\frac{\tau_\beta v}{s^{2-\beta}}\frac{1}{\tau_{\min\{\alpha,\beta\}}s^{\min\{\alpha,\beta\}}}\right\} \tag{B3}$$

and

$$\langle x^2(t)\rangle = \mathscr{L}^{-1}\left\{\left[\frac{2(1-\beta)\tau_\beta v^2}{s^{3-\beta}} + \frac{2\sigma^2}{s}\right]\frac{1}{\tau_{\min\{\alpha,\beta\}}s^{\min\{\alpha,\beta\}}} + \frac{2\beta\tau_\beta^2 v^2 s^{2\beta-3}}{\tau^2_{\min\{\alpha,\beta\}}s^{2\min\{\alpha,\beta\}}}\right\}. \tag{B4}$$

The following calculations on MSD should take care of the value of α and β.

For $\alpha > \beta$, after invoking Eq. (A11), we can get the asymptotic behavior of the first moment $\langle x(t)\rangle$ and second moment $\langle x^2(t)\rangle$, which can be expressed as

$$\langle x(t)\rangle \simeq vt \tag{B5}$$

and

$$\langle x^2(t)\rangle \simeq v^2t^2 + \frac{2\sigma^2}{\Gamma(1+\beta)\tau_\beta}t^\beta. \tag{B6}$$

Correspondingly, it is

$$\langle \Delta x^2(t)\rangle = \langle x^2(t)\rangle - \langle x(t)\rangle^2 = \frac{2\sigma^2}{\Gamma(1+\beta)\tau_\beta}t^\beta. \tag{B7}$$

For $\alpha < \beta$, similarly, after invoking Eq. (A14), we have

$$\langle x(t)\rangle \simeq \frac{\tau_\beta v}{\Gamma(2+\alpha-\beta)\tau_\alpha}t^{1+\alpha-\beta} \tag{B8}$$

and

$$\langle x^2(t)\rangle \simeq \frac{2(1-\beta)\tau_\beta v^2}{\Gamma(3+\alpha-\beta)\tau_\alpha}t^{2+\alpha-\beta} + \frac{2\sigma^2}{\Gamma(1+\alpha)\tau_\alpha}t^\alpha + \frac{2\beta\tau_\beta^2 v^2}{\Gamma(3+2\alpha-2\beta)\tau_\alpha^2}t^{2+2\alpha-2\beta}. \tag{B9}$$

Correspondingly, it is

$$\langle \Delta x^2(t)\rangle = \frac{2(1-\beta)\tau_\beta v^2}{\Gamma(3+\alpha-\beta)\tau_\alpha}t^{2+\alpha-\beta} + \frac{2\sigma^2}{\Gamma(1+\alpha)\tau_\alpha}t^\alpha + \frac{\tau_\beta^2 v^2}{\tau_\alpha^2}\left[\frac{2\beta}{\Gamma(3+2\alpha-2\beta)} - \frac{1}{\Gamma^2(2+\alpha-\beta)}\right]t^{2+2\alpha-2\beta}. \tag{B10}$$

It can be seen that $\sim t^{2+\alpha-\beta}$ is the leading term of Eq. (B10), hence the MSD can be approximately expressed as

$$\langle \Delta x^2(t)\rangle \simeq \frac{2(1-\beta)\tau_\beta v^2}{\Gamma(3+\alpha-\beta)\tau_\alpha} t^{2+\alpha-\beta} \tag{B11}$$

at a large timescale.

2. Other cases

For $1 < \alpha < 2$ and $1 < \beta < 2$, similar to the calculations in Eq. (B2), from Eq. (B1) we can arrive at

$$P(k,s) \simeq \frac{1}{s}\frac{(T_\alpha + T_\beta)s - i(\beta-1)\tau_\beta v s^{\beta-1}k - bs^{\beta-2}k^2}{(T_\alpha + T_\beta)s + iT_\beta vk + ds^{\beta-2}k^2 + \sigma^2 k^2}. \tag{B12}$$

Correspondingly, the first moment $\langle x(t)\rangle$ and second moment $\langle x^2(t)\rangle$ can be approximately expressed by

$$\langle x(t)\rangle \simeq \frac{T_\beta v}{T_\alpha + T_\beta} t + \frac{(\beta-1)\tau_\beta v}{\Gamma(3-\beta)(T_\alpha + T_\beta)} t^{2-\beta} \tag{B13}$$

and

$$\langle x^2(t)\rangle \simeq \frac{T_\beta^2 v^2}{(T_\alpha + T_\beta)^2} t^2 + \frac{2(\beta-1)(T_\alpha + 2T_\beta)\tau_\beta v^2}{\Gamma(4-\beta)(T_\alpha + T_\beta)^2} t^{3-\beta} + \frac{2\sigma^2}{T_\alpha + T_\beta} t, \tag{B14}$$

respectively. From Eqs. (B13) and (B14), it can be seen that $\sim t^{3-\beta}$ is the leading term in expressing the MSD at the long-time limit.

For $0 < \alpha < 1$ and $1 < \beta < 2$, the propagator can be expressed as

$$P(k,s) \simeq \frac{1}{s}\frac{\tau_\alpha s^\alpha - i(\beta-1)\tau_\beta v s^{\beta-1}k - bs^{\beta-2}k^2}{\tau_\alpha s^\alpha + iT_\beta vk + ds^{\beta-2}k^2 + \sigma^2 k^2}, \tag{B15}$$

and

$$\langle x(t)\rangle \simeq \frac{(\beta-1)\tau_\beta v}{\Gamma(2+\alpha-\beta)\tau_\alpha} t^{1+\alpha-\beta} + \frac{T_\beta v}{\Gamma(1+\alpha)\tau_\alpha} t^\alpha, \tag{B16}$$

$$\langle x^2(t)\rangle \simeq \frac{2(\beta-1)\tau_\beta v^2}{\Gamma(3+\alpha-\beta)\tau_\alpha} t^{2+\alpha-\beta} + \frac{2T_\beta^2 v^2}{\Gamma(1+2\alpha)\tau_\alpha^2} t^{2\alpha} + \frac{2(\beta-1)T_\beta \tau_\beta v^2}{\Gamma(2+2\alpha-\beta)\tau_\alpha^2} t^{1+2\alpha-\beta} + \frac{2\sigma^2}{\Gamma(1+\alpha)\tau_\alpha} t^\alpha. \tag{B17}$$

From Eqs. (B16) and (B17), it can be seen that $\sim t^{2+\alpha-\beta}$ $(2-\beta > \alpha)$ or $\sim t^{2\alpha}$ $(2-\beta < \alpha)$ is the leading term in expressing the MSD at the long-time limit.

For $1 < \alpha < 2$ and $0 < \beta < 1$, the propagator can be expressed as

$$P(k,s) \simeq \frac{1}{s}\frac{\tau_\beta s^\beta + i(\beta-1)\tau_\beta v s^{\beta-1}k - bs^{\beta-2}k^2}{\tau_\beta s^\beta + i\beta\tau_\beta v s^{\beta-1}k + ds^{\beta-2}k^2 + \sigma^2 k^2} \tag{B18}$$

and

$$\langle x(t)\rangle \simeq vt, \tag{B19}$$

$$\langle x^2(t)\rangle \simeq v^2 t^2 + \frac{2\sigma^2}{\Gamma(1+\beta)\tau_\beta} t^\beta. \tag{B20}$$

From Eqs. (B19) and (B20), it can be seen that the MSD $\langle \Delta x^2(t)\rangle \sim t^\beta$ which is a subdiffusion.

APPENDIX C: DETAILS OF NUMERICAL SIMULATION

Generation of the waiting times and jump times: We choose $\omega_r(t) = \alpha\tau_0^\alpha t^{-(1+\alpha)}, t \geqslant \tau_0$ and $\omega_j(t) = \beta\tau_0^\beta t^{-(1+\beta)}, t \geqslant \tau_0$, and $\tau_0 = 1$ for the numerical simulations. The two random time intervals are both generated as follows. First, a random variable ξ_1 with a uniform distribution in the interval [0,1] is seeded, from which a random variable τ is constructed in simulation as

$$\tau = \tau_0(1-\xi_1)^{-1/\alpha}. \tag{C1}$$

The required random time interval is then provided by τ for $\tau \geqslant \tau_0$, and 0 otherwise.

Generation of the jump lengths: The Gaussian-distributed jump length can be generalized by using the Box-Müller method,

$$x = \sqrt{-2\sigma^2 \ln\xi_2}\cos(2\pi\xi_3), \tag{C2}$$

in which ξ_2 and ξ_3 are the random variables with the uniform distribution in the interval [0,1].

Generations of the LW steps: In numerical simulations, we choose the velocity as $v = 1$ and $v = -1$ with equal probability, and the excursion in each LW step is simply the product of the velocity and jump time.

Numerical scheme: We initially release the random walker at $x = 0$. The evolving time is $t = m\Delta t$, where $m = 0, 1,$

2, ..., M, $M = 10^8$, and $\Delta t = 10^{-3}$ is a constant time interval between two consecutive recordings. The walker initially enters the CTRW state. For the CTRW state, to record and iterate the process, we followed the scheme introduced by Ref. [37] (see Fig. 1 of Ref. [37] for a very nice schematic description on the CTRW renewal process), e.g., the walker first completes a waiting time; once the evolving time exceeds the present waiting time, an instantaneous jump length is generated and recorded and the walker then enters the LW state. For the LW state, the iterations are much simpler—the coordinate of the random walker is iterated with $v\Delta t$. Once the evolving time exceeds the present jump time, the iteration terminates and the walker enters the CTRW state. The process iterates.

[1] E. W. Montroll and G. H. Weiss, J. Math. Phys. **6**, 167 (1965).
[2] H. Scher and E. W. Montroll, Phys. Rev. B **12**, 2455 (1975).
[3] R. Kutner and J. Masoliver, Eur. Phys. J. B: Topic Issue **90**, 50 (2017).
[4] J.-P. Bouchaud and A. Georges, Phys. Rep. **195**, 127 (1990).
[5] R. Metzler and J. Klafter, Phys. Rep. **339**, 1 (2000).
[6] R. Metzler, J. H. Jeon, A. G. Cherstvy, and E. Barkai, Phys. Chem. Chem. Phys. **16**, 24128 (2014).
[7] V. Zaburdaev, S. Denisov, and J. Klafter, Rev. Mod. Phys. **87**, 483 (2015).
[8] J. Klafter and I. M. Sokolov, *First Steps in Random Walks. From Tools to Applications* (Oxford University Press, Oxford, 2011).
[9] E. Barkai, Y. Garini, and R. Metzler, Phys. Today **65**(8), 29 (2012).
[10] F. Höfling and T. Franosch, Rep. Prog. Phys. **76**, 046602 (2013).
[11] I. Golding and E. C. Cox, Phys. Rev. Lett. **96**, 098102 (2006).
[12] S. C. Weber, A. J. Spakowitz, and J. A. Theriot, Phys. Rev. Lett. **104**, 238102 (2010).
[13] J.-H. Jeon, V. Tejedor, S. Burov, E. Barkai, C. Selhuber-Unkel, K. Berg-Sørensen, L. Oddershede, and R. Metzler, Phys. Rev. Lett. **106**, 048103 (2011).
[14] J. Szymanski and M. Weiss, Phys. Rev. Lett. **103**, 038102 (2009).
[15] B. Berkowitz, I. Dror, S. K. Hansen, and H. Scher, Rev. Geophys. **54**, 930 (2016).
[16] A. Cortis and B. Berkowitz, Soil. Sci. Soc. Am. J. **68**, 1539 (2004).
[17] M. Levy and B. Berkowitz, J. Contam. Hydrol. **64**, 203 (2003).
[18] B. Bijeljic, P. Mostaghimi, and M. J. Blunt, Phys. Rev. Lett. **107**, 204502 (2011).
[19] D. Froemberg, M. Schmiedeberg, E. Barkai, and V. Zaburdaev, Phys. Rev. E **91**, 022131 (2015).
[20] M. Magdziarz and T. Zorawik, Phys. Rev. E **95**, 022126 (2017).
[21] A. Kamińska and T. Srokowski, Phys. Rev. E **96**, 032105 (2017).
[22] A. Kamińska and T. Srokowski, Phys. Rev. E **97**, 062120 (2018).
[23] A. Dechant and E. Lutz, Phys. Rev. Lett. **108**, 230601 (2012).
[24] D. A. Kessler and E. Barkai, Phys. Rev. Lett. **108**, 230602 (2012).
[25] G. Margolin and E. Barkai, Phys. Rev. Lett. **94**, 080601 (2005).
[26] G. Margolin and E. Barkai, J. Chem. Phys. **121**, 1566 (2004).
[27] G. Ariel, A. Rabani, S. Benisty, J. D. Partridge, R. M. Harshey, and A. Be'er, Nat. Commun. **6**, 8396 (2015).
[28] P. Barthelemy, P. J. Bertolotti, and D. S. Wiersma, Nature (London) **453**, 495 (2008).
[29] M. Buchanan, Nature (London) **453**, 714 (2008).
[30] J. Klafter and G. Zumofen, Phys. Rev. E **49**, 4873 (1994).
[31] V. Zaburdaev and K. Chukbar, JETP **94**, 252 (2002).
[32] T. H. Solomon, E. R. Weeks, and H. L. Swinney, Phys. Rev. Lett. **71**, 3975 (1993).
[33] M. S. Song, H. C. Moon, J.-H. Jeon, and H. Y. Park, Nat. Commun. **9**, 344 (2018).
[34] M. A. Lomholt, T. Koren, R. Metzler, and J. Klafter, Proc. Natl. Acad. Sci. USA **105**, 11055 (2008).
[35] O. Bénichou, C. Loverdo, M. Moreau, and R. Voituriez, Rev. Mod. Phys. **83**, 81 (2011).
[36] W. Wang and E. Barkai, Phys. Rev. Lett. **125**, 240606 (2020).
[37] E. Heinsalu, M. Patriarca, I. Goychuk, G. Schmid, and P. Hänggi, Phys. Rev. E **73**, 046133 (2006).
[38] M. Schmiedeberg, V. Y. Zaburdaev, and H. Stark, J. Stat. Mech. (2009) P12020.
[39] One can prove that in calculating Eqs. (16) and (17), if the jump length of the CTRW state is not taken into account, e.g., $\sigma = 0$, the expression of MSD is exactly the first term of the right-hand side of Eq. (17), and if the ballistic excursion of the LW state is not taken into account, e.g., $v = 0$, the expression of MSD is exactly the second one. Besides, it can be seen that v^2 is only contained in the expression of D_1 and D_2, and σ^2 is only contained in the expression of D_1' and D_2'.
[40] A. Bodrova, A. K. Dubey, S. Puri, and N. Brilliantov, Phys. Rev. Lett. **109**, 178001 (2012).
[41] T. K. Haxton and A. J. Liu, Europhys. Lett. **90**, 66004 (2010).
[42] J. Liu, J. D. Bao, and X. S. Chen, Phys. Rev. E **102**, 062122 (2020).
[43] J. Liu, C. Y. Zhang, J. D. Bao, and X. S. Chen, Soft Matter **17**, 9786 (2021).
[44] F. F. Li, P. Zhu, J. D. Bao, X. S. Chen, and J. Liu, J. Stat. Mech. (2021) 043210.
[45] F. Etoc, E. Balloul, C. Vicario, D. Normanno, D. Liße, A. Sittner, J. Piehler, M. Dahan, and M. Coppey, Nat. Mater. **17**, 740 (2018).
[46] C. P. Brangwynne, G. H. Koenderink, F. C. MacKintosh, and D. A. Weitz, Trends Cell Biol. **19**, 423 (2009).
[47] M. Guo, A. J. Ehrlicher, M. H. Jensen, M. Renz, J. R. Moore, R. D. Goldman, J. Lippincott-Schwartz, F. C. Mackintosh, and D. A. Weitz, Cell **158**, 822 (2014).
[48] C. Leduca, K. Padberg-Gehlec, V. Vargaa, D. Helbinge, S. Dieza, and J. Howarda, Proc. Natl. Acad. Sci. **109**, 6100 (2012).
[49] N. Hirokawa, S. Niwa, and Y. Tanaka, Neuron **68**, 610 (2010).
[50] The case $0 < \mu < 1$, though very similar, is not considered here.
[51] Strictly speaking, for Lévy flight, the variance diverges and cannot be directly calculated, an alternative method is to introduce an imagery box which spans the spatial interval $[-Lt^{1/\mu}, Lt^{1/\mu}]$, which gives a method to measure the MSD: $\langle x^2(t)\rangle_L = \int_{-Lt^{1/\mu}}^{Lt^{1/\mu}} x^2 P(x,t)dx$, see Phys. Rev. E **59**, 2736 (1999). We applied this method in calculating and expressing Eq. (21).

[52] A. Compte, Phys. Rev. E **55**, 6821 (1997).
[53] A. Compte, R. Metzler, and J. Camacho, Phys. Rev. E **56**, 1445 (1997).
[54] B. R. Parry, I. V. Surovtsev, M. T. Cabeen, C. S. O'Hern, E. R. Dufresne, and C. Jacobs-Wagner, Cell **156**, 183 (2014).
[55] J. S. Leith, A. Tafvizi, F. Huang, W. E. Uspal, P. S. Doyle, A. R. Fersht, L. A. Mirny, and A. M. van Oijen, Proc. Natl. Acad. Sci. USA **109**, 16552 (2012).
[56] T. Miyaguchi, T. Akimoto, and E. Yamamoto, Phys. Rev. E **94**, 012109 (2016).
[57] T. Miyaguchi, T. Uneyama, and T. Akimoto, Phys. Rev. E **100**, 012116 (2019).
[58] X. Wang, Y. Chen, and W. Deng, Phys. Rev. E **100**, 012136 (2019).
[59] X. Wang, Y. Chen, and W. Deng, Phys. Rev. Research **2**, 013102 (2020).